Journal of Oil Palm Research Vol. 35 (1) March 2023 p. 86-99
DOI: https://doi.org/10.21894/jopr.2022.0048

COMPARISON OF ARTIFICIAL INTELLIGENCE MODELS TO PREDICT OIL PALM BIOMASS PYROLYSIS AND KINETICS USING THERMOGRAVIMETRIC ANALYSIS

YASMIN MOHD ZAIFULLIZAN[1]; LIM MEI KUAN[2]; ARSHAD ADAM SALEMA[1,3]* and KASHIF ISHAQUE[4]

ABSTRACT

Kinetic modeling is a challenging aspect of biomass conversion due to its inherent complex reactions. Further, it is difficult to achieve the accuracy of predicting the biomass pyrolysis process at varying experimental conditions, particularly for more complex samples based on kinetic modeling alone. Therefore, this study aims to use artificial intelligence (AI) models [artificial neural network (ANN), support vector machine (SVM), and decision tree (DT)] to predict biomass thermogravimetric (TG) behaviour, derivative TG (DTG), product (volatile and char) yield, and kinetic triplets. Two oil palm biomass types-empty fruit bunches (EFB) and oil palm shells (OPS) - are used to generate a 72-experiment dataset from a thermogravimetric analyser (TGA) at different heating rates (5°C, 10°C, 15°C and 20°C min^{-1}). The results reveal that each AI model can accurately predict the DTG profile with high coefficients of determination (R^2) in the range of 0.94 and 0.99 and low mean square errors (MSE) between 0.09 and 5.12. The product yield prediction results are not as promising, as indicated by higher MSE values (4.27, 2.79, 6.67). However, the ANN models most capably predicted the activation energies of oil palm biomass pyrolysis (~260°C-360°C at 20°C min^{-1}) for both model-free and model-fitting methods, followed by the DT and SVM models.

Keywords: artificial intelligence, kinetics, oil palm biomass, pyrolysis, thermogravimetric.

Received: 1 January 2022; **Accepted:** 4 July 2022; **Published online:** 11 August 2022.

INTRODUCTION

Biomass pyrolysis is regarded as one of the most promising alternative methods for producing three different products; solid (char), liquid (bio-oil), and gas. It is a complex multi-scale process due to several interactive and parallel reactions that require further research work (Sharifzadeh *et al.*, 2019). One of the main challenges is that the pyrolysis process and product formation (yield and quality) performance depend strongly on process/operating conditions (Chen *et al.*, 2017; Guedes *et al.*, 2018; Mutsengerere *et al.*, 2019; Paenpong and Pattiya, 2016). It was found that pyrolysis temperature and heating rate play an essential role during pyrolysis and product formation (Guedes *et al.*, 2018; Sharifzadeh *et al.*, 2019). Moreover, feedstock properties and chemical complexity add to the difficulty of the problem. These factors make it difficult to understand the kinetic modeling of biomass pyrolysis (Cai *et al.*, 2018; Hameed *et al.*, 2019; Hu and Gholizadeh, 2019; Kaczor *et al.*, 2020; Wang *et al.*, 2017).

[1] Mechanical Engineering Discipline, School of Engineering, Monash University Malaysia, 47500 Bandar Sunway, Selangor, Malaysia.

[2] School of Information Technology, Monash University Malaysia, 47500 Bandar Sunway, Selangor, Malaysia.

[3] Monash Industry Palm Oil Research Platform (MIPO), School of Engineering, Monash University Malaysia, 47500 Bandar Sunway, Malaysia.

[4] Electrical and Computer Engineering, Mohammad Ali Jinnah University, 194823 Karachi, Sindh, Pakistan.

* *Corresponding author e-mail: arshad.salema@monash.edu*

The kinetic triplet, namely activation energy, pre-exponential factor and reaction model or mechanism helps to describe the complex thermal degradation process that can be beneficial for subsequent processes and applications (Mahmood *et al.*, 2019). The kinetic triplet of biomass pyrolysis is obtained by varying the heating rates during thermogravimetric analysis (TGA) and model-free methods such as the Flynn-Wall-Ozawa (FWO), Kissinger-Akihara-Sunose (KAS), and Friedman methods are employed (Zhang *et al.*, 2021). Model-fitting method such as the Coats-Redfern method is utilised as well with the added benefit of being able to hypothesize reaction mechanisms for the process. For example, Castells *et al.* (2021) presented a preliminary view that empty fruits bunch (EFB) samples showed a better fit for the diffusion reactions, while oil palm shell (OPS) and palm mesocarp fibre (PMF) could better fit n-order reactions under a combustion scheme. Surahmanto *et al.* (2020) applied the Coats-Redfern integral method for kinetic analysis of oil palm waste and found that they are best fitted to first-order reactions in the pyrolysis scheme.

Traditionally, biomass pyrolysis reaction is modelled using kinetic models (Hameed *et al.*, 2019). Kinetic models have been developed for decades and give useful insight into the reaction kinetics of biomass pyrolysis. Examples of kinetic models include the one-step global kinetic model (Papari and Hawboldt, 2015), parallel (Radmanesh *et al.*, 2006) and competitive (Várhegyi *et al.*, 1997) reactions, lumped kinetic models and the distributed activation energy model (DAEM) (Ahmad *et al.*, 2020) which mainly focus on primary reactions of pyrolysis. Although much effort has been put into investigating pyrolytic kinetic models, it is still difficult to capture the full complexity of the biomass structure and the interdependence of the individual components (Wang *et al.*, 2017). It is recommended that rather than modeling a singular biomass component *e.g.*, cellulose, it is better to model the whole biomass to observe the interactions between the different components and the possible effects of trace amounts of inorganic materials, as well as to include secondary reactions from the process (Hameed *et al.*, 2019).

Meanwhile, there has been an increasing interest in applying AI to the biomass conversion process in recent years. Several machine learning (ML) algorithms were recently applied to biomass pyrolysis (Alaba *et al.*, 2020; Aydinli *et al.*, 2017; Chen *et al.*, 2018; Ding *et al.*, 2020; Rezk *et al.*, 2019). Most of these studies have used artificial neural networks (ANN) and concluded that they could predict the pyrolysis process with high accuracy due to their ability to discover hidden patterns in complex data (Alaba *et al.*, 2020). Further, ANN was used to model TGA experimental datasets due to its capability to handle: (i) large datasets from TGA systems (>10 000 data samples per run); (ii) the complex non-linear nature of thermal conversion, and; (iii) fully automated modeling procedures (Teng *et al.*, 2019). Besides biomass, researchers have also applied ANN to sewage sludge (Naqvi *et al.*, 2018) and co-pyrolysis of sewage sludge with rice husk (Lakovic *et al.*, 2021; Naqvi *et al.*, 2019). Others have predicted the higher heating values of biomass using a hybrid adaptive neuro-fuzzy inference system (ANFIS) (Pattanayak *et al.*, 2020) and ANN (Çakman *et al.*, 2021).

Although AI models have been used to predict biomass pyrolysis behaviour (weight loss using TG curve), very few (Bhuyan *et al.*, 2020) have been applied to predict product yield (gas/volatile components and char). Furthermore, a few studies have used a support vector machine (SVM) involving biomass pyrolysis. For instance, Cao *et al.* (2016) and Ewees *et al.* (2017) applied SVM to predict the biochar yield from cattle manure. Another study by Chen *et al.* (2018) computed the product distribution and bio-oil heating value of different biomasses under fast pyrolysis using SVM. The studies on applying decision trees (DT) to biomass pyrolysis are even more scarce. For example, Zhang *et al.* (2019) applied random forest, a DT ensemble methwangod, to cattle manure pyrolysis, while Zhu *et al.* (2019) predicted biochar yields and carbon contents using random forest. Although some researchers have applied AI to biomass pyrolysis, few studies (Aghbashlo *et al.*, 2021) have provided a detailed investigation of kinetic parameter prediction such as activation energy using AI methods. To date, none have utilised and compared different AI models (ANN, SVM and DT) for biomass pyrolysis based on real-time data obtained from a TGA machine. It is hypothesised that AI would save significant time and effort by predicting the biomass pyrolysis behaviour as compared to time-consuming experimental procedures with TGA machines.

The objective of the present work is to develop, train, validate, and compare three AI models to predict the pyrolysis behaviour, kinetics, and product yield of two oil palm biomasses; EFB and OPS. The datasets were generated using a TGA machine at different heating rates and then used to develop and compare the performance of three AI models. The scope of this work also includes developing AI models based on individual biomass pyrolysis datasets and combining them. Another novelty of the present work is extracting the activation energy from the predicted values obtained by AI models. It should be noted that although the developed AI models are specific to oil palm biomass (OPS and EFB), it is expected that they would also work for other types of biomasses having a similar pyrolysis conversion trend.

MATERIALS AND METHODS

Materials

This study used OPS and EFB obtained from local palm oil mills in Malaysia. The biomasses were cleaned, dried in the open sun and then grounded to smaller-sized particles in the range of 75-250 µm to mitigate heat transfer effects (Wei *et al.*, 2006). Finally, the biomasses were stored in airtight Ziplock bags for further analysis. The proximate and ultimate analyses of the biomasses (*Table 1*) confirmed that EFB and OPS are different in chemical properties and exhibit different pyrolysis behaviours. The ultimate analyses were conducted with a Leco CHNS analyser model 932 (The Netherlands) according to ASTM D5373-14 and ISO 29541 method, and the analysis was repeated five times for each sample expressed as the dry basis of biomass.

TABLE 1. PROXIMATE AND ULTIMATE ANALYSIS OF OIL PALM BIOMASS

Proximate analysis (wt.%)		
	EFB	**OPS**
Moisture content (M)	6.10 ± 2.10	7.43 ± 1.98
Volatile matter (VM)	80.00 ± 1.00	73.5 ± 0.85
Ash (A)	5.80 ± 0.70	2.20 ± 0.80
Fixed carbon[#]	8.10 ± 0.75	16.87 ± 0.95
Ultimate analysis (%), dry basis		
C	47.26 ± 0.85	51.07 ± 1.18
H	5.83 ± 0.01	4.71 ± 0.25
N	0.82 ± 0.03	0.41 ± 0.02
S	<0.05	<0.05
O*	46.04	43.76

Note: [#]Fixed carbon is by difference = 100 - [M + VM + A] %.
*Oxygen is by difference, % = 100 – [C + H + N + S] %.

Thermogravimetric Analysis (TGA)

The experiments were conducted in a thermogravimetric analyser (TA Instrument Q50, USA). About 5-7 mg of biomass sample (EFB or OPS, respectively) was placed in a ceramic pan and loaded into the TGA in each experiment. The temperature was ramped from room temperature to maximum temperatures of 400°C, 450°C and 500°C, at different heating rates (β) of 5°C, 10°C, 15°C and 20°C min^{-1} in an inert (nitrogen) environment under a 60 mL min^{-1} constant gas flow rate. The maximum temperature of 400°C, 450°C and 500°C was selected as the biomass gets completely pyrolysed before 400°C. Lower heating rates are recommended (Vyazovkin *et al.*, 2011) to prevent thermal lag (by ensuring effective heat and mass transfer in the sample) so that the temperature error can be minimised or eliminated. Each experiment was conducted three times to guarantee data reproducibility.

Artificial Neural Network (ANN) Modeling

Six different ANN models (*e.g.,* OPS TG - Oil palm shell thermogravimetric; EFB DTG - Empty fruit bunch derivative thermogravimetric; OPS+EFB TG - Oil palm shell and EFB combined thermogravimetric) were trained and optimised for pyrolysis behaviour (TG and DTG curves). The first four models (OPS TG, OPS DTG, EFB TG, and EFB DTG) are based on individual biomass pyrolysis datasets with temperature and heating rate as the input, while the combined ANN models use OPS+EFB datasets that increase the complexity of the non-linear relationships.

The architecture was a typical multi-layer feed-forward backpropagation neural network consisting of an input layer, one hidden layer, and an output layer, known as a shallow neural network (*Figure 1a*). The input layer data consists of temperature and heating rate, while the output layer data were the TG curve, DTG curve, or product yield. The data from the TG machine performed under the heating rate of 20°C min^{-1} and temperature of 400°C was set aside for validation *i.e.*, 20%. The remaining data (80%) was used to train the model. The ANN parameters such as the training and transfer functions and the number of neurons in the hidden layer were optimised by trial and error to obtain the minimum mean square error (MSE). The performance of the ANN models is evaluated by calculating the MSE and coefficient of determination (R^2). Lower MSE values and higher R^2 values indicate better ANN model performance.

The product yield ANN models also used shallow neural networks (one input layer, one hidden layer, and one output layer). The only difference was that the output layer comprised the two different yields (volatiles and char) from the pyrolysis process. Two ANN models, one for each biomass (OPS and EFB), were developed to predict the yield.

Support Vector Machine (SVM) Modeling

The SVM algorithm is much faster and requires a smaller sample size than other machine learning algorithms (Russell and Norvig, 2016). Similar to ANN, six SVM regression models (*Figure 1b*) were created. The dataset was split into training and validation datasets in an 80:20 ratio. A kernel transforms the predictor variables to a higher-dimensional feature space. The Gaussian function was selected for this work due to its popularity and accuracy for regression (Arabloo *et al.*, 2015).

Decision Tree (DT) Modeling

DT has gained popularity due to its ease of interpretability and simplicity. DT follows a flowchart-like tree structure (*Figure 1c*), governed by decision rules similar to 'if-then' conditions, making it easily understandable (Myles *et al.*, 2004). DT has the advantage of requiring less training time than ANN and SVM. Like the ANN and SVM models, six DT models (or regression trees) were created for TG and DTG curves. The dataset for DT was split into an 80:20 ratio for training and validation. The optimised hyperparameters were branch nodes, leaf sizes, and tree depth, determined empirically to minimise the five-fold cross-validation loss (Myles *et al.*, 2004). All simulations were performed with MATLAB (R2018b, Version 9.5) on an Intel® Core™ i5-4570S, 16 GB RAM, 2.90 GHz processor, and Windows 10 64-bit operating system.

Kinetic and Reaction Mechanism Study

The kinetic triplets-activation energy (E_a), pre-exponential factor (A), and reaction model were evaluated in the main pyrolysis region based on the TG data. The activation energy is interpreted as the minimum energy threshold for a reaction to occur (Truhlar, 1978). The pre-exponential factor is the pre-exponential constant in the Arrhenius equation, an empirical relationship between temperature and rate coefficient (Jagannadham, 2010), which is used to study the reaction mechanism. Lastly, the reaction model or the reaction mechanism is the account of elementary reactions by which chemical change occurs in a compound (Smith and March, 2013). Model-free methods, such as the Flynn-Wall-Ozawa (FWO), Kissinger-Akihara-Sunose (KAS), and Friedman methods, were used to determine the kinetic parameters (Zhang *et al.*, 2021). In addition, the Coats-Redfern (CR) model-fitting method was adopted to determine the activation energy (E_a), pre-exponential factor (A) and reaction model by plotting versus (Chen *et al.*, 2019). If the value obtained by the CR model-fitting method based on a specific reaction model is comparable to the average obtained by the model-free methods (Friedman, FWO, and KAS), the reaction model is considered suitable for characterising the corresponding thermal degradation process (Chen *et al.*, 2019).

The trained ANN, SVM, and DT models were used to predict the TG data in the validation step. The activation energies and pre-exponential factors of the oil palm biomasses were then calculated from these predicted TG data using different kinetic methods (FWO, KAS, and Friedman). Finally, the predicted kinetic data were compared with those obtained from the experimental TG dataset.

RESULTS AND DISCUSSION

Thermogravimetric Analysis of OPS and EFB Biomass Samples

The TG and DTG profiles obtained at different heating rates and temperatures of OPS and EFB biomass pyrolysis showed some notable differences as shown in *Figure 2*. The first stage or peak from room temperature to 200°C corresponds to the removal of moisture and probably low volatile or

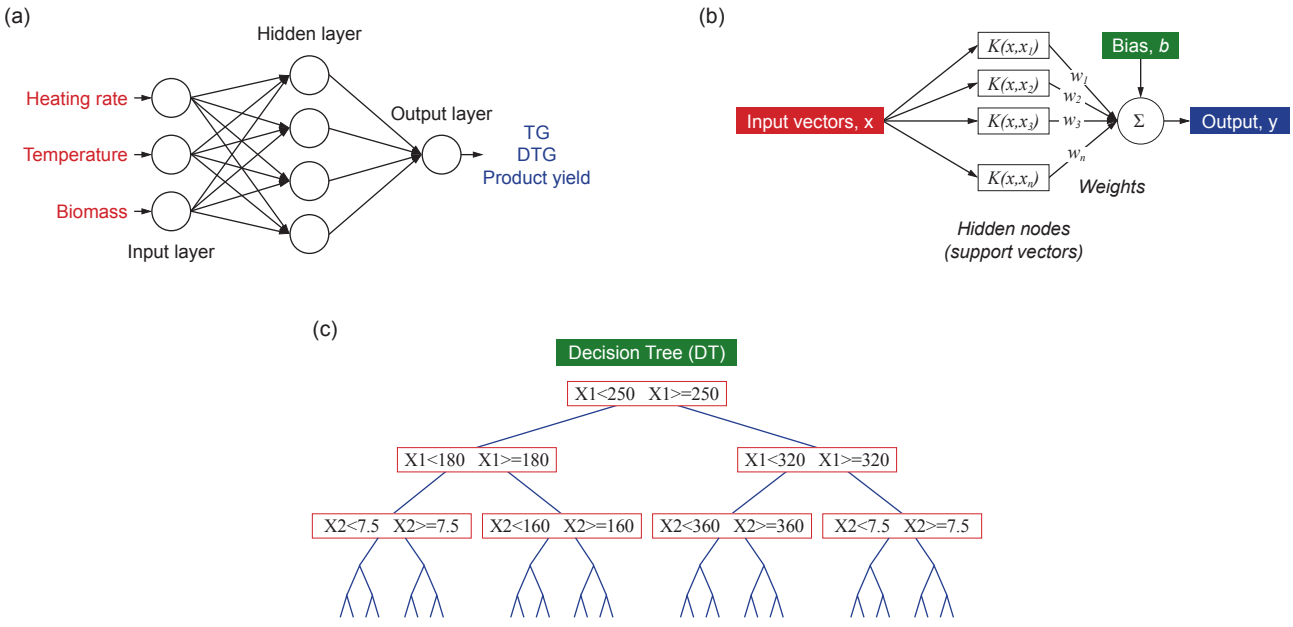

Figure 1. (a) ANN, (b) SVM, and (c) DT architecture to predict the oil palm biomass pyrolysis behaviour and product yield.

chemical compounds. The second stage between 200°C and 380°C is referred to as the main pyrolysis reaction stage in which cellulose and hemicellulose are decomposed to release volatile matter. A clear difference between hemicellulose (shoulder peak) and cellulose decomposition is identified in OPS biomass whereas it is almost absent in EFB biomass due to the lower content of hemicellulose (Abdullah and Gerhauser, 2008). The third stage is attributed to the char formation that occurs once all the volatile matter has been emitted (below 400°C) and denotes the completion of biomass pyrolysis. This can be observed by a gradual loss in weight after 380°C and usually, lignin decomposes in this region. Among the lignocellulosic materials, lignin is a stable component that has low reactivity. It decomposes slowly over a wide range of temperatures and can simultaneously decompose with hemicellulose and cellulose. A significant difference in pyrolysis behaviour (TG and DTG curves) was observed in the main decomposition region or second stage while the curves tend to merge in the char region or third stage. The derivative mass loss rate of EFB is higher than OPS due to the swift burning of volatile matter in form of cellulose (Asadieraghi and Daud, 2015).

As the heating rate increased, the DTG curves shifted to higher temperatures. This is in agreement with previous studies of non-isothermal heating (Yıldız *et al.*, 2016). The observed shift may be explained by the mathematical form of kinetic laws as explained by Janković *et al.* (2020). Typically, reaction intensity increases when the heating rate is increased thereby accelerating the devolatilisation process. However, the char formation stage gets delayed with the increase in heating rate. At lower heating rates, samples are heated more gradually with a low-temperature gradient, resulting in better

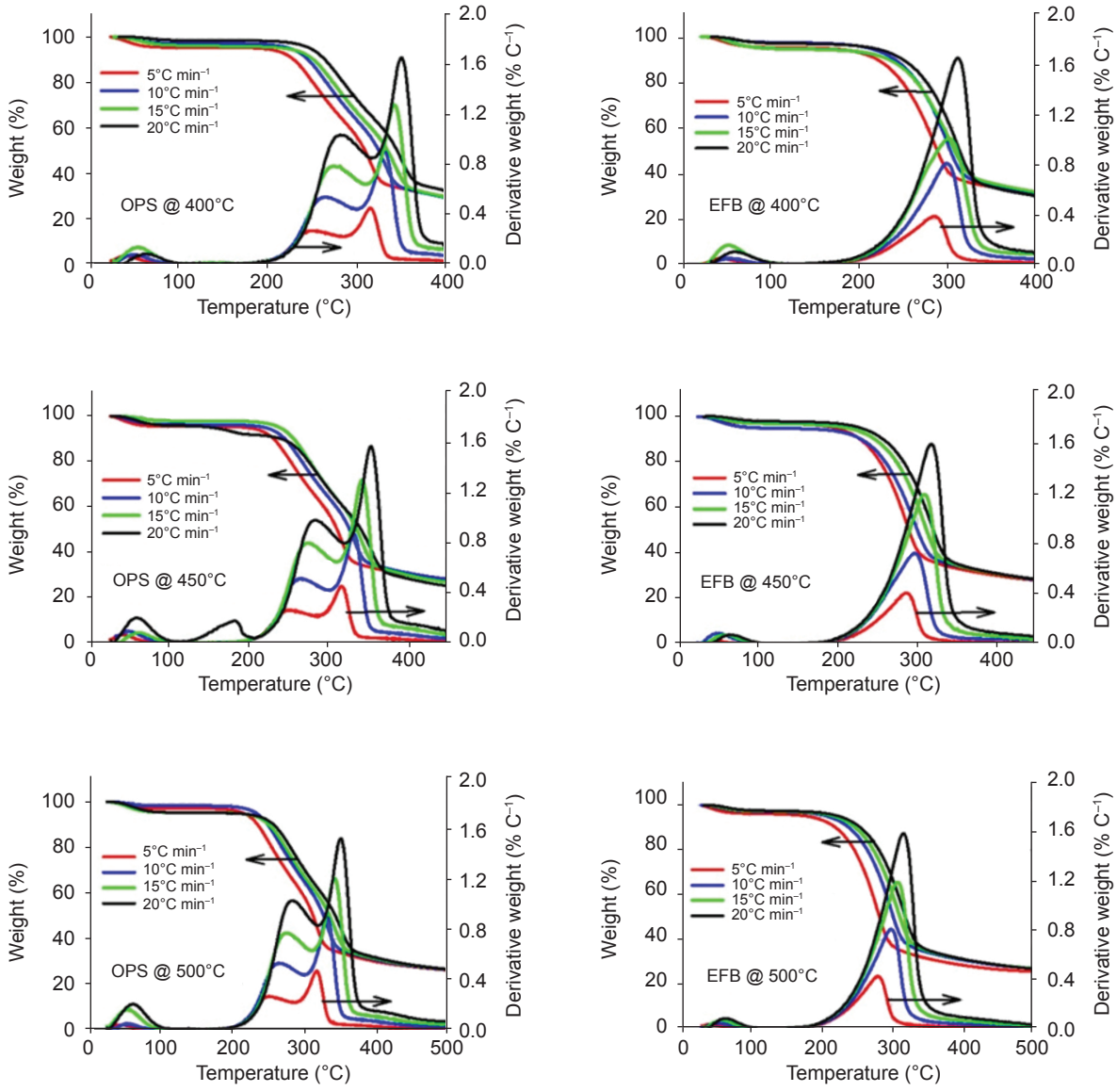

Figure 2. TG and DTG profiles of OPS and EFB biomass at different temperatures and heating rates.

heat transfer from the surface of the particles to the inner core. However, the high-temperature gradient is developed at higher heating rates resulting in reaction retardation. The TGA of OPS and EFB agrees with the previously published literature (Asadieraghi and Daud, 2015; Luangkiattikhun *et al.*, 2008), and hence, limited discussion is presented in this article.

Prediction of Biomass Pyrolysis Behaviour (TG-DTG) Using Different AI Models

Table 2 presents the performance of the AI model predictions of the pyrolysis behaviour (TG/DTG profiles) of oil palm biomass. The training columns represent the model performance after being trained, while the validation columns represent the model performance on the dataset not used in the training phase. *Figure 3* presents the predicted and the experimental TG and DTG profiles suggesting that the shape of the curves predicted by all the AI models followed the degradation curves from the experimental data. Overall, the accuracy of all the models was high. There was a strong agreement between the targeted and predicted output ($R^2 > 0.99$) for both the validation and training datasets.

The average R^2 values for both individual and combined ANN models training TG dataset was 0.999, indicating extremely high agreement between the measured and predicted results. For the validation TG dataset, the average R^2 values decreased slightly to 0.996. The average R^2 values for the DTG training and validation datasets were somewhat lower than for the TG dataset at 0.994 and 0.967, respectively.

On the other hand, the average MSE for both individual and combined ANN models were 0.77 for the training TG dataset and 3.94 for the validation dataset. In comparison, the average MSE values for the DTG training and validation dataset were 0.03 and 0.98, respectively. These MSE values show that the errors between the target and output values were minor for the training ANN models, indicating a well-trained model. However, there are significant differences between the ANN model training and validation MSE values for the TG and DTG predictions. The lower value of the MSE (below 1.0) for the DTG demonstrates the robustness of the ANN model. The difference in R^2 for the TG and DTG predictions is minor, which agrees with a previous study (Alaba *et al.*, 2020). The performance of the present ANN model was comparable to previous studies (*Table 2*). The performance of previous studies (Bi *et al.*, 2020; 2021; Naqvi *et al.*, 2019) were limited to TG data only. To the best of the author's knowledge, only one study (Zhang *et al.*, 2019) on DT was found whereby they obtained a DT model with R^2 of 0.9996 and RMSE of 0.501 for cattle manure. Meanwhile, no study was found on SVM, as SVM and DT were applied for the first time to predict the oil palm biomass pyrolysis behaviour.

However, the findings of the current study which suggest that ANN performs better than SVM and DT do not support some previous research. For instance, Cao *et al.* (2016) concluded that SVM predicted cattle manure pyrolysis better than the ANN model. Another study (Chen *et al.*, 2018) reported a similar SVM prediction outcome for biomass pyrolysis. This inconsistency may be due to the data used because cattle manure and oil palm biomass have different compositions and

TABLE 2. PERFORMANCE ANALYSIS OF ANN, SVM AND DT MODELS TO PREDICT PYROLYSIS BEHAVIOUR OF BIOMASS

Dataset	Parameters	AI models						
		ANN			SVM		DT	
		Training	Validation*	Comparison with literature	Training	Validation*	Training	Validation*
OPS TG	R^2	0.99	0.99	R^2 = 0.99992, RMSE = 0.3561 for sewage sludge and peanut shell TG (Bi *et al.*, 2021)	0.99	0.99	0.99	0.99
	MSE	0.51	2.79		3.10	3.28	0.53	2.97
OPS DTG	R^2	0.99	0.98		0.99	0.99	0.99	0.99
	MSE	0.02	0.43		0.03	0.09	0.02	0.39
EFB TG	R^2	0.99	0.99	R^2 = 0.99995, RMSE = 0.5194 for coal gangue and biomass TG (Bi *et al.*, 2020)	0.99	0.99	0.99	0.99
	MSE	1.02	5.04		1.25	5.09	1.05	5.11
EFB DTG	R^2	0.99	0.94		0.99	0.95	0.99	0.97
	MSE	0.04	1.56		0.06	1.34	0.04	1.58
OPS+EFB TG	R^2	0.99	0.99	R^2 = 0.9996, RMSE = 0.5142 for rice husk and sewage sludge TG (Naqvi *et al.*, 2019)	0.99	0.99	0.99	0.99
	MSE	0.77	3.99		0.96	4.90	0.81	4.21
OPS+EFB DTG	R^2	0.99	0.96		0.99	0.96	0.99	0.98
	MSE	0.03	0.93		0.04	0.97	0.03	0.98

Note: *Validation dataset for temperature 400°C and heating rate 20°C min^{-1}.

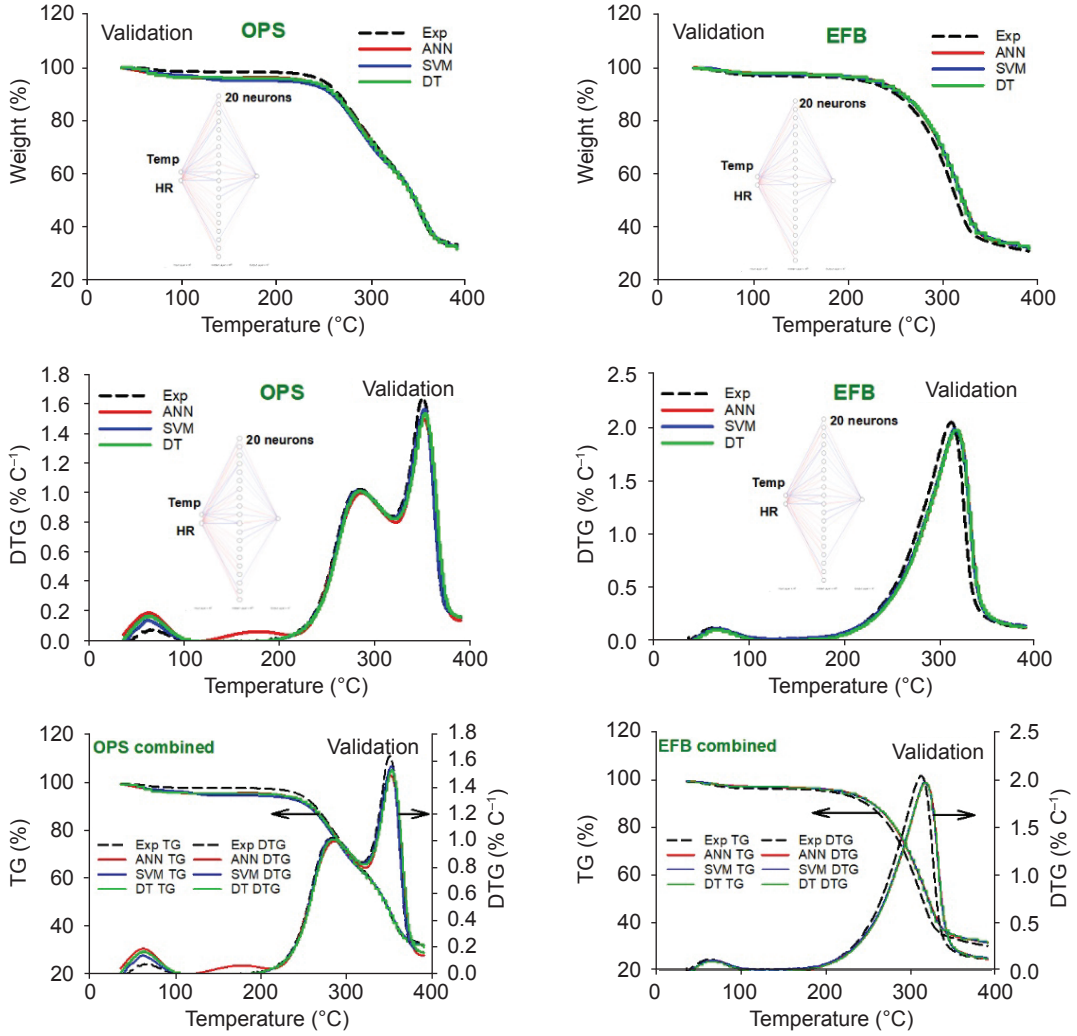

Figure 3. Comparison of ANN, SVM and DT validation models to predict the TG and DTG (derivative thermogravimetric) profiles of OPS and EFB biomass pyrolysis at a maximum temperature of 400°C and heating rate of 20°C min^{-1}.

thermal behaviour. Data collection and the size of the datasets also differ. For example, Chen *et al.* (2018) used data from previously published studies and collected 166 samples of various lignocellulosic biomass fast pyrolysis. Although the present results differ from some published studies (Cao *et al.*, 2016; Chen *et al.*, 2018), they are consistent with studies that have applied AI to biomass pyrolysis using TGA (Alaba *et al.*, 2020; Chen *et al.*, 2018; Yıldız *et al.*, 2016).

Another critical parameter to evaluate the performance of the AI models is training time. The average times to train the ANN, SVM, and DT models were 100, 319 and 87 s, respectively. The training time is highly dependent on the dataset size and computer hardware configuration. SVM took considerably more time for training, while DT trained the fastest. Although training the ANN network takes more time than DT, the TG and DTG predictions by the ANN are more accurate. Therefore, it can be concluded that ANN is the best performing algorithm for TG and DTG datasets since it provides a good trade-off between high accuracy (R^2), low error (MSE), and a reasonable training time (100 s). It is also worth noting that the AI system obtains validation results in approximately 2 s, which is faster than the time needed to perform real-time TGA experiments by a factor of 1000, which usually take hours to complete from laboratory preparation to clean up. Most studies in the field of AI application in biomass pyrolysis have failed to present the AI training time, which is one of the vital parameters in determining performance.

Application of ANN, SVM and DT Models to Predict Pyrolysis Product Yield

The yields of two major pyrolysis products (volatile and biochar) were obtained from the TG curves (*Figure 3*) by referring to the different stages of decomposition (Janković *et al.*, 2020). The product yield does not include the moisture content.

Pyrolysis product heating rate or temperature trends were not noticeable (*Figure 4*). Similar findings were reported in previous studies (Wang *et al.*, 2013; 2019). A possible reason for this could be the small sample size (5-7 mg) used in the TGA machine, ensuring efficient heat transfer. For the volatile and char yield training datasets, the ANN, SVM and DT models showed low MSE values of 0.17, 0.01 and 0.94, respectively. However, the MSE values for the ANN (4.27), SVM (2.79), and DT (6.67) models were higher for the validation set. This prediction (validation) result error is due to the small data sample size.

The MSE value of 5.171 for the ANN model testing datasets to predict the product yields of biomass pyrolysis was higher (Aydinli *et al.*, 2017) than the present ANN model product validation dataset. However, the present ANN (4.27) and SVM (2.79) model validation MSE values were almost similar to the root mean squared error (RMSE) of the ANN model (3.35-4.50) testing dataset and SVM model (2.53-3.34) testing dataset (Chen *et al.*, 2018). Therefore, the developed AI models in the present study are either slightly better or comparable to the previous studies.

Figure 4 compares the validation and measured product (volatile and char) yield using the ANN, SVM, and DT models. Contrary to the prediction results for pyrolysis (TG and DTG), the models moderately predicted the product yield percentage. The AI models either slightly over-predicted or under-predicted the product yield. The models' performance could be improved by increasing the dataset size.

Application of the ANN, SVM and DT Models to Predict Activation Energy and Pre-exponential Factor

The ANN predictions for in the main pyrolysis temperature range, (260°C-360°C) of OPS biomass was highly accurate for both model-free methods (KAS and FWO), as illustrated in *Figure 5*. The SVM prediction was accurate for OPS in the temperature range from 260°C to 305°C (from 10% to 40% conversion). Beyond 305°C, *i.e.*, after 40% conversion, the SVM over-predicted by an average factor of 1.17 for KAS and 1.16 for FWO. Surprisingly, all AI models predicted lower than the experimental data for the KAS and FWO methods for EFB biomass with an average factor of 0.91. This deviation in the prediction of could be due to the predicted TG profiles, since any deviation in the predicted TG profiles would change the values.

The value of from the KAS method first increased from ~100 kJ mol^{-1} (10% conversion) to 119 kJ mol^{-1} (60% conversion) for OPS biomass and then remained nearly constant (119 kJ mol^{-1}) until 90% conversion. The trend was similar for the FWO method but with a slightly higher values (~103 kJ mol^{-1} for 10% conversion to 122 kJ mol^{-1} for 60% conversion) for OPS biomass. The variation in in the main pyrolysis, the region is due to the decomposition of hemicellulose in the initial stage of the reaction, followed by degradation of cellulose with higher thermal stability starting in the later reaction (Wang *et al.*, 2019).

The DT model provided a much more accurate predictions, agreeing with the experimental values except for a small spike at 50% and 40% conversion for OPS and EFB biomass, respectively (*Figure 5*). These spikes could be due to a slight discrepancy in the DT model prediction of the TG profile (*Figure 3*) that may have caused the prediction to diverge. For the EFB biomass, the DT prediction of yielded a slightly higher error against experimental values compared to the ANN and SVM.

The average experimental and predicted activation energies for OPS and EFB biomass in the main pyrolysis region between 260°C and 330°C are presented in *Table 3*. It should be noted that the average activation energy and standard deviation refer to a value between 0.1 to 0.9 conversion degrees. Further, the average experimental value for OPS from the combined kinetic model-free methods (KAS, FWO, and Friedman) is 122 kJ

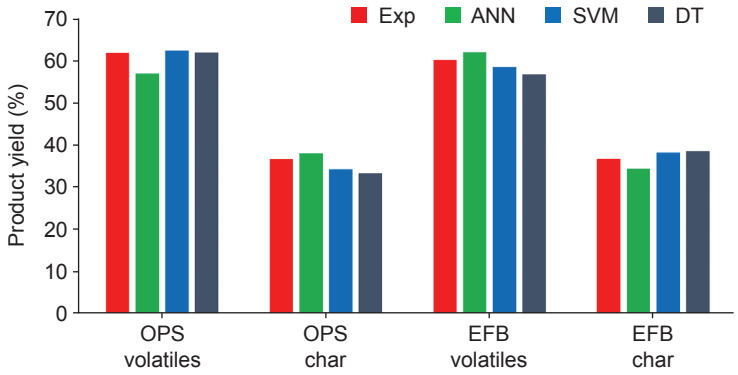

Figure 4. Performance of AI models in predicting the biomass pyrolysis product (volatiles and char) yield at 400°C and heating rate of 20°C min^{-1}.

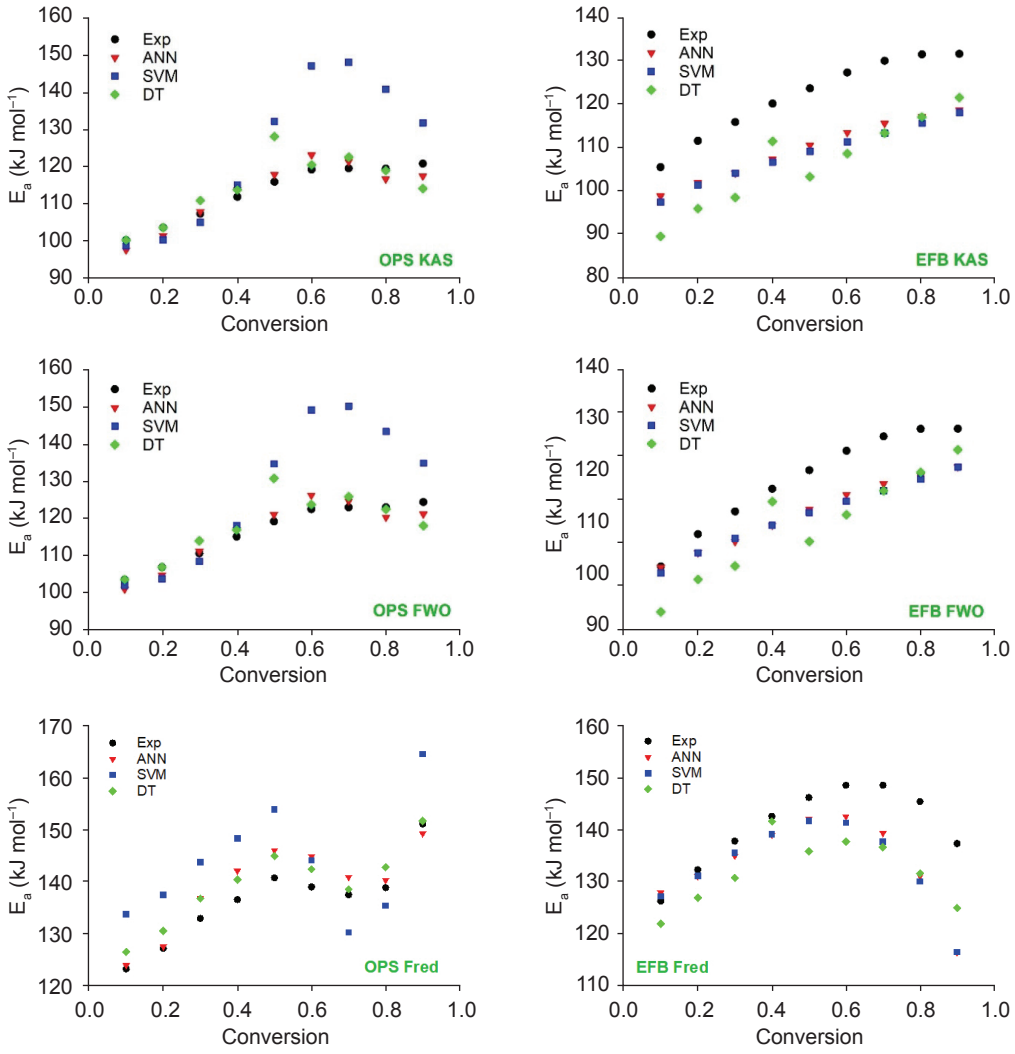

Figure 5. Comparison of extracted activation energy (E_a) using ANN, SVM and DT with experimental values.

mol^{-1} with a standard deviation of ±13, while the average for the ANN, SVM and DT are 122, 132, and 124 kJ mol^{-1} with standard deviations of ±14, ±10, and ±13, respectively. Whereas the average experimental for EFB from the combined kinetic model-free methods (KAS, FWO, and Friedman) is 127 kJ mol^{-1} with a standard deviation of 12. The average for the ANN, SVM and DT models are 119, 118, and 116 kJ mol^{-1} with standard deviations of 13, 14, and 14, respectively.

Therefore, for the OPS biomass, the error (%) between the average experimental and predicted activation energies for the ANN, DT, and SVM models were ~1%, ~2% and ~10%, respectively. For the EFB biomass, the corresponding errors were ~7%, ~10%, and ~8%, respectively. The change in activation energy with conversion degree was confirmed by previous studies (Huang *et al.*, 2019). They reported a 4% error between the predicted and experimental activation energy using a general regression neural network (GRNN) model. To conclude, among the AI models, ANN most accurately predicts the TG and DTG behaviour and biomass pyrolysis kinetics. The error between the experimental and predicted values from the FWO calculation method were lower, agreeing with very recently published work (Bong *et al.*, 2020).

Prediction of Reaction Mechanism Using the Model-fitting Method

In the present study, the values based on the CR method were compared with KAS and FWO model-free methods since the Friedman method provided higher values. The reaction mechanism was selected as the most suitable mechanism to characterise OPS and EFB pyrolysis when the values obtained from the CR method are closest to model-free methods. *Tables 4* and *5* show the comparison of values and pre-exponential factors from the experiment and AI models for OPS and EFB at a heating rate of 20°C min^{-1}, along with correlation coefficient and the average deviations between the results from the AI models and the experimental calculations.

On average, OPS AI models E_a and ln A deviated 6.48 kJ mol^{-1} and 1.38 from the calculated values obtained from the experiment. For EFB, the deviations were 7.01 kJ mol^{-1} and 1.57 for E_a and ln A, respectively. The biggest deviation for both OPS and EFB was for the decision tree model, while ANN showed the smallest deviation from the experimental values.

The experimental values of 102, 109, and 128 kJ mol^{-1} (*Table 4*) for OPS biomass corresponding to reaction model numbers 2 (chemical reaction), 6 (1st order reaction), and 7 (nucleation), respectively, is closest to KAS (113 kJ mol^{-1}) and FWO (116 kJ mol^{-1}). The values of the corresponding correlation coefficient were higher (0.8) for reaction models 2 and 6 but lower (0.7) for reaction model 7. For the EFB (*Table 5*), reaction models 1 (chemical reaction) and 9 (contracting disk) gave the closest experimental values of 137 and 131 kJ mol^{-1}, respectively, compared to KAS (119 kJ mol^{-1}) and FWO (122 kJ mol^{-1}). The values of the correlation coefficient were higher (0.8) in both cases. Zhang *et al.* (2021) pointed out that applying multiple model-free methods is more accurate than a single method for solid-state pyrolysis.

TABLE 3. COMPARISON OF PREDICTED AND EXPERIMENTAL AVERAGE ACTIVATION ENERGIES

Kinetic models	Experiment and AI models	Activation energies, kJ mol^{-1}			
		OPS		EFB	
		Average$^{\#}$	Stdev*	Average$^{\#}$	Stdev*
KAS	Experiment	113.01	7.75	118.77	9.51
	ANN	112.90	8.89	109.56	7.07
	SVM	124.26	19.97	108.38	6.78
	DT	114.64	8.96	106.40	10.50
FWO	Experiment	116.47	7.80	121.69	9.33
	ANN	116.37	8.84	112.32	6.87
	SVM	127.14	19.35	111.83	6.74
	DT	118.02	8.84	109.96	10.25
Friedman	Experiment	136.28	8.09	140.57	7.77
	ANN	139.02	8.50	133.8	8.40
	SVM	143.48	10.94	133.34	8.17
	DT	139.35	7.58	131.96	6.55

Note: $^{\#}$Average - average activation energy from 0.1-0.9 conversion degree.
*Stdev - standard deviation (±).

TABLE 4. COMPARISON OF ACTIVATION ENERGIES AND PRE-EXPONENTIAL FACTOR OBTAINED FROM EXPERIMENT AND AI MODELS USING COATS-REDFERN METHOD FOR OPS*

Reaction models	Experiment			ANN			SVM			DT			The average deviation from experimental values	
	R^2	E_a (kJ mol^{-1})	ln A	R^2	E_a (kJ mol^{-1})	ln A	R^2	E_a (kJ mol^{-1})	ln A	R^2	E_a (kJ mol^{-1})	ln A	E_a (kJ mol^{-1})	ln A
1	0.79	90.15	12.67	0.79	92.21	13.10	0.82	94.89	13.75	0.87	79.50	10.41	5.82	1.26
2	0.84	102.15	14.44	0.84	103.94	14.81	0.87	108.80	15.95	0.91	90.95	12.07	6.55	1.42
3	0.63	64.36	8.00	0.63	66.56	8.19	0.65	66.07	8.11	0.72	53.80	5.42	4.82	0.96
4	0.53	52.33	5.21	0.53	54.44	5.67	0.54	53.23	5.42	0.61	41.66	2.85	4.56	1.01
5	0.45	43.69	3.35	0.45	45.70	3.80	0.46	44.21	3.47	0.51	33.00	0.93	4.41	1.00
6	0.87	109.07	17.76	0.86	112.13	18.07	0.90	118.74	19.59	0.92	98.80	15.26	7.67	1.55
7	0.70	128.09	20.59	0.76	131.34	21.29	0.79	133.53	21.81	0.85	112.36	17.31	8.14	1.73
8	0.77	36.25	1.48	0.70	37.34	1.72	0.73	38.07	1.92	0.79	31.00	0.27	2.72	0.63
9	0.75	82.17	11.22	0.75	84.34	11.68	0.78	85.80	12.05	0.83	71.67	8.99	5.43	1.17
10	0.81	94.65	13.42	0.81	96.63	13.83	0.84	105.76	14.65	0.89	83.85	11.13	7.96	1.31
11	0.83	99.55	14.14	0.83	101.40	14.52	0.86	100.08	15.54	0.90	88.51	11.80	4.47	1.37
12	0.77	174.01	29.83	0.77	178.35	30.72	0.79	181.27	31.44	0.85	153.03	25.50	10.86	2.28
13	0.78	42.49	2.66	0.77	43.48	2.88	0.81	45.21	3.31	0.86	37.08	1.44	3.04	0.70
14	0.75	164.87	25.52	0.75	169.16	26.40	0.77	171.40	26.97	0.84	143.89	21.18	10.60	2.22
15	0.71	148.03	21.61	0.71	152.23	22.48	0.73	153.26	22.78	0.80	127.08	17.27	10.13	2.13

Note: *E_a and ln A calculations are based on temperature 400°C and heating rate 20°C min^{-1}.

TABLE 5. COMPARISON OF ACTIVATION ENERGIES AND PRE-EXPONENTIAL FACTOR OBTAINED FROM EXPERIMENT AND AI MODELS USING COATS-REDFERN METHOD FOR EFB*

Reaction models	Experiment			ANN			SVM			DT			Average deviation from experimental values	
	R^2	E_a (kJ mol^{-1})	ln A	R^2	E_a (kJ mol^{-1})	ln A	R^2	E_a (kJ mol^{-1})	ln A	R^2	E_a (kJ mol^{-1})	ln A	E_a (kJ mol^{-1})	ln A
1	0.88	136.86	23.53	0.75	141.19	24.43	0.89	136.80	23.43	0.96	124.22	20.69	5.68	1.28
2	0.92	153.42	26.36	0.92	151.22	25.77	0.92	151.33	25.79	0.97	137.48	22.76	6.74	1.59
3	0.76	102.67	16.67	0.77	104.50	17.02	0.77	105.18	17.17	0.88	93.09	14.53	4.64	1.00
4	0.68	87.03	13.36	0.70	89.32	13.84	0.70	90.04	13.99	0.82	77.51	11.24	4.94	1.08
5	0.61	75.65	10.92	0.63	78.35	11.49	0.64	78.80	11.59	0.76	65.88	8.723	5.21	1.15
6	0.93	165.37	30.48	0.93	161.37	29.48	0.93	161.54	29.51	0.98	146.41	26.20	8.93	2.08
7	0.86	193.84	35.67	0.86	194.80	35.77	0.86	195.32	35.88	0.94	177.12	31.97	6.39	1.34
8	0.83	61.03	7.51	0.84	58.70	6.92	0.84	58.88	6.96	0.93	52.80	5.58	4.24	1.02
9	0.85	131.37	22.64	0.86	126.75	21.52	0.86	127.10	21.59	0.94	114.96	18.95	8.43	1.95
10	0.90	143.02	24.66	0.77	146.80	25.43	0.90	142.26	24.40	0.96	129.29	21.57	6.09	1.37
11	0.91	149.79	25.81	0.78	152.96	26.44	0.91	148.19	25.35	0.97	134.67	22.41	6.63	1.50
12	0.86	272.07	52.10	0.87	262.85	49.89	0.87	263.55	50.03	0.95	239.28	44.86	16.84	3.84
13	0.88	66.84	8.56	0.88	66.32	8.40	0.89	66.46	8.43	0.92	59.97	6.96	2.59	0.63
14	0.84	249.47	44.78	0.85	251.22	45.02	0.85	251.94	45.17	0.94	227.52	39.96	8.72	1.82
15	0.81	227.14	39.62	0.82	229.69	40.05	0.82	230.46	40.21	0.92	205.73	34.93	9.09	1.90

Note: *E_a and ln A calculations are based on temperature 400°C and heating rate 20°C min^{-1}.

The lower R^2 value for the reaction models of OPS biomass (0.7) as compared to EFB (0.8) can be related to the DTG profile of OPS (*Figure 3*). It clearly shows two reaction peaks in the main devolatilisation region which indicates that the single-step approach may not be accurate in investigating the kinetic triplets, and a multi-step reaction model should be considered (Guo and Lua, 2001; Luangkiattikhun *et al.*, 2008). In contrast, the DTG profile of EFB (*Figure 3*) showed a single reaction peak.

Interestingly, among the AI models, the ANN model most accurately predicted values and pre-exponential factors compared to the experimental values using the CR kinetic method, followed by the SVM and DT models. Although the ANN and SVM models predicted values closer to the experimental dataset, the DT model predicted lower values. It was also observed that the predictions of the E_a and pre-exponential factor values also depend on the type of reaction mechanism. As discussed, the R^2 is lower for most of the reaction mechanisms, indicating that not all reaction mechanisms accurately represent the thermal degradation of oil palm biomass.

CONCLUSION

For the first time, three different AI models (ANN, SVM and DT) were used to predict pyrolysis behaviour, kinetic parameters, and the product yield of oil palm biomass using TGA. Interestingly, all three AI models accurately predicted the biomass pyrolysis behaviour with low MSE values between 0.09 and 5.11 and high R^2 values between 0.949 and 0.999. This study also permitted the extraction of kinetic parameters (activation energy, pre-exponential factor, and reaction model) from the predicted TG data and compared them to experimental data. The ability of the ANN model to predict pyrolysis behaviour, kinetic parameters, and biomass product yield demonstrates the robustness of the algorithm in obtaining the most promising results compared to the SVM and DT models. The ANN displayed high regression coefficients (R^2), low MSE values, and a reasonable training period (100 s). The performance of the developed AI models was slightly better or at least comparable in terms of MSE values to the existing AI models in the literature. AI models promise to become a powerful tool to predict biomass pyrolysis behaviour and kinetic parameters to avoid tedious and lengthy TGA experiments.

ACKNOWLEDGEMENT

This project was financially supported by the Ministry of Higher Education, Malaysia, under the Fundamental Research Grant Scheme (FRGS) No. FRGS/1/2018/TK10/MUSM/03/1. Author is also grateful to Monash University Malaysia campus for the graduate scholarship.

REFERENCES

Abdullah, N and Gerhauser, H (2008). Bio-oil derived from empty fruit bunches. *Fuel, 87(12)*: 2606-2613.

Aghbashlo, M; Almasi, F; Jafari, A; Nadian, M H; Soltanian, S; Lam, S S and Tabatabaei, M (2021). Describing biomass pyrolysis kinetics using a generic hybrid intelligent model: A critical stage in sustainable waste-oriented biorefineries. *Renew. Energy*, *170*: 81-91. DOI: 10.1016/j.renene.2021.01.111.

Ahmad, M S; Liu, H; Alhumade, H; Tahir, M H; Çakman, G; Yıldız, A; Ceylan, S; Elkamel, A and Shen, B (2020). A modified DAEM: To study the bioenergy potential of invasive Staghorn Sumac through pyrolysis, ANN, TGA, kinetic modeling, FTIR and GC–MS analysis. *Energy Convers. Manag., 221*: 113173.

Alaba, P A; Popoola, S I; Abnisal, F; Lee, C S; Ohunakin, O S; Adetiba, E; Akanle, M B; Abdul Patah, M F; Atayero, A A A and Wan Daud, W M A (2020). Thermal decomposition of rice husk: A comprehensive artificial intelligence predictive model. *J. Therm. Anal. Calorim., 140(4)*: 1811-1823. DOI: 10.1007/s10973-019-08915-0.

Arabloo, M; Ziaee, H; Lee, M and Bahadori, A (2015). Prediction of the properties of brines using least squares support vector machine (LS-SVM) computational strategy. *J. Taiwan Inst. Chem. Eng., 50*: 123-130. DOI: 10.1016/j.jtice.2014.12.005.

Asadieraghi, M and Daud, W M A W (2015). In-depth investigation on thermochemical characteristics of palm oil biomasses as potential biofuel sources. *J. Anal. Appl. Pyrolysis, 115*: 379-391.

Aydinli, B; Caglar, A; Pekol, S and Karaci, A (2017). The prediction of potential energy and matter production from biomass pyrolysis with artificial neural network. *Energ. Explor. Exploit., 35(6)*: 698-712. DOI: 10.1177/0144598717716282.

Bhuyan, N; Narzari, R; Bujar Baruah, S M and Kataki, R (2020). Comparative assessment of artificial neural network and response surface methodology for evaluation of the predictive capability on bio-oil yield of *Tithonia diversifolia* pyrolysis. *Biomass Convers. Biorefin.,*: 1-16. DOI: 10.1007/s13399-020-00806-x.

Bi, H; Wang, C; Jiang, X; Jiang, C; Bao, L and Lin, Q (2021). Thermodynamics, kinetics, gas emissions and artificial neural network modeling of co-pyrolysis of sewage sludge and peanut shell. *Fuel, 284:* 118988. DOI: 10.1016/j.fuel.2020.118988.

Bi, H; Wang, C; Lin, Q; Jiang, X; Jiang, C and Bao, L (2020). Combustion behavior, kinetics, gas emission characteristics and artificial neural network modeling of coal gangue and biomass via TG-FTIR. *Energy, 213*: 118790. DOI: 10.1016/j.energy.2020.118790.

Bong, J T; Loy, A C M; Chin, B L F; Lam, M K; Tang, D K H; Lim, H Y; Chai, Y H and Yusup, S (2020). Artificial neural network approach for co-pyrolysis of *Chlorella vulgaris* and peanut shell binary mixtures using microalgae ash catalyst. *Energy, 207*: 118289. DOI: 10.1016/j.energy.2020.118289.

Cai, J; Xu, D; Dong, Z; Yu, X; Yang, Y; Banks, S W and Bridgwater, A V (2018). Processing thermogravimetric analysis data for isoconversional kinetic analysis of lignocellulosic biomass pyrolysis: Case study of corn stalk. *Renew. Sustain. Energy Rev., 82*: 2705-2715. DOI: 10.1016/J.RSER.2017.09.113.

Çakman, G; Gheni, S and Ceylan, S (2021). Prediction of higher heating value of biochars using proximate analysis by artificial neural network. *Biomass Convers. Biorefin.,*: 1-9. DOI: 10.1007/s13399-021-01358-4.

Cao, H; Xin, Y and Yuan, Q (2016). Prediction of biochar yield from cattle manure pyrolysis via least squares support vector machine intelligent approach. *Bioresour. Technol., 202*: 158-164. DOI: 10.1016/j.biortech.2015.12.024.

Castells, B; Amez, I; Medic, L and García-Torrent, J (2021). Torrefaction influence on combustion kinetics of Malaysian oil palm wastes. *Fuel Process. Technol., 218*: 106843. DOI: 10.1016/j.fuproc.2021.106843.

Chen, H; Liu, J; Chang, X; Chen, D; Xue, Y; Liu, P; Lin, H and Han, S (2017). A review on the pretreatment of lignocellulose for high-value chemicals. *Fuel Process. Technol., 160*: 196-206. DOI: 10.1016/j.fuproc.2016.12.007.

Chen, R; Li, Q; Xu, X and Zhang, D (2019). Pyrolysis kinetics and reaction mechanism of representative non-charring polymer waste with micron particle size. *Energy Convers. Manag., 198*: 111923. DOI: 10.1016/J.ENCONMAN.2019.111923.

Chen, X; Zhang, H; Song, Y and Xiao, R (2018). Prediction of product distribution and bio-oil heating value of biomass fast pyrolysis. *Chem. Eng. Process.: Process Intensif., 130*: 36-42. DOI: 10.1016/j.cep.2018.05.018.

Ding, Y; Huang, B; Li, K; Du, W; Lu, K and Zhang, Y (2020). Thermal interaction analysis of isolated hemicellulose and cellulose by kinetic parameters during biomass pyrolysis. *Energy*, *195*: 117010. DOI: 10.1016/j.energy.2020.117010.

Ewees, A A; Aziz, M A E l and Elhoseny, M (2017). Social-spider optimization algorithm for improving ANFIS to predict biochar yield. *2017 8th International Conference on Computing, Communication and Networking Technologies (ICCCNT)*. Delhi, India. p. 1-6. DOI: 10.1109/ICCCNT.2017.8203950.

Guedes, R E; Luna, A S and Torres, A R (2018). Operating parameters for bio-oil production in biomass pyrolysis: A review. *J. Anal. Appl. Pyrolysis*, *129*: 134-149. DOI: 10.1016/J.JAAP.2017.11.019.

Guo, J and Lua, A C (2001). Kinetic study on pyrolytic process of oil-palm solid waste using two-step consecutive reaction model. *Biomass Bioenergy*, *20(3)*: 223-233. DOI: 10.1016/S0961-9534(00)00080-5.

Hameed, S; Sharma, A; Pareek, V; Wu, H and Yu, Y (2019). A review on biomass pyrolysis models: Kinetic, network and mechanistic models. *Biomass Bioenergy*, *123*: 104-122. DOI: 10.1016/j.biombioe.2019.02.008.

Hu, X and Gholizadeh, M (2019). Biomass pyrolysis: A review of the process development and challenges from initial researches up to the commercialisation stage. *J. Energy Chem.*, *39*: 109-143. DOI: 10.1016/j.jechem.2019.01.024.

Huang, Y W; Chen, M Q and Li, Q H (2019). Artificial neural network model for the evaluation of chemical kinetics in thermally induced solid-state reaction. *J. Therm. Anal. Calorim.*, *138(1)*: 451-460. DOI: 10.1007/s10973-019-08232-6.

Jagannadham, V (2010). How do we introduce the Arrhenius pre-exponential factor (A) to graduate students? *Creat.*, *1(2)*: 128. DOI: 10.4236/ce.2010.12019.

Janković, B; Manić, N and Stojiljković, D (2020). The gaseous products characterization of the pyrolysis process of various agricultural residues using TGA–DSC–MS techniques. *J. Therm. Anal. Calorim.*, *139(5)*: 3091-3106. DOI: 10.1007/s10973-019-08733-4.

Kaczor, Z; Buliński, Z and Werle, S (2020). modeling approaches to waste biomass pyrolysis: A review. *Renew. Energy*, *159*: 427-443. DOI: 10.1016/j.renene.2020.05.110.

Kan, T; Strezov, V and Evans, T J (2016). Lignocellulosic biomass pyrolysis: A review of product properties and effects of pyrolysis parameters. *Renew. Sustain. Energy Rev.*, *57*: 1126-1140. DOI: 10.1016/J.RSER.2015.12.185.

Lakovic, N; Khan, A; Petković, B; Petkovic, D; Kuzman, B; Resic, S; Jermsittiparsert, K and Azam, S (2021). Management of higher heating value sensitivity of biomass by hybrid learning technique. *Biomass Convers. Biorefin.* p. 1-8. DOI: 10.1007/s13399-020-01223-w.

Luangkiattikhun, P; Tangsathitkulchai, C and Tangsathitkulchai, M (2008). Non-isothermal thermogravimetric analysis of oil-palm solid wastes. *Bioresour. Technol.*, *99(5)*: 986-997. DOI: 10.1016/J.BIORTECH.2007.03.001.

Mahmood, H; Moniruzzaman, M; Iqbal, T; Yusup, S; Rashid, M and Raza, A (2019). Comparative effect of ionic liquids pretreatment on thermogravimetric kinetics of crude oil palm biomass for possible sustainable exploitation. *J. Mol. Liq.*, *282*: 88-96. DOI: 10.1016/j.molliq.2019.02.133.

Mutsengerere, S; Chihobo, C H; Musademba, D and Nhapi, I (2019). A review of operating parameters affecting bio-oil yield in microwave pyrolysis of lignocellulosic biomass. *Renew. Sustain. Energy Rev.*, *104*: 328-336. DOI: 10.1016/j.rser.2019.01.030.

Myles, A J; Feudale, R N; Liu, Y; Woody, N A and Brown, S D (2004). An introduction to decision tree modeling. *J. Chemom.*, *18(6)*: 275-285. DOI: 10.1002/cem.873.

Naqvi, S R; Hameed, Z; Tariq, R; Taqvi, S A; Ali, I; Niazi, M B K; Noor, T; Hussain, A; Iqbal, N and Shahbaz, M (2019). Synergistic effect on co-pyrolysis of rice husk and sewage sludge by thermal behavior, kinetics, thermodynamic parameters and artificial neural network. *Waste Manage.*, *85*: 131-140. DOI: 10.1016/j.wasman.2018.12.031.

Naqvi, S R; Tariq, R; Hameed, Z; Ali, I; Taqvi, S A; Naqvi, M; Niazi, M B K; Noor, T and Farooq, W (2018). Pyrolysis of high-ash sewage sludge: Thermo-kinetic study using TGA and artificial neural networks. *Fuel*, *233*: 529-538. DOI: 10.1016/j.fuel.2018.06.089.

Paenpong, C and Pattiya, A (2016). Effect of pyrolysis and moving-bed granular filter temperatures on the yield and properties of bio-oil from fast pyrolysis of biomass. *J. Anal. Appl. Pyrolysis*, *119*: 40-51. DOI: 10.1016/j.jaap.2016.03.019.

Papari, S and Hawboldt, K (2015). A review on the pyrolysis of woody biomass to bio-oil: Focus on kinetic models. *Renew. Sust. Energ. Rev., 52*: 1580-1595.

Pattanayak, S; Loha, C; Hauchhum, L and Sailo, L (2020). Application of MLP-ANN models for estimating the higher heating value of bamboo biomass. *Biomass Convers. Bioref., 11*: 2499-2508. DOI: 10.1007/s13399-020-00685-2.

Radmanesh, R; Courbariaux, Y; Chaouki, J and Guy, C (2006). A unified lumped approach in kinetic modeling of biomass pyrolysis. *Fuel, 85(9)*: 1211-1220.

Rezk, H; Nassef, A M; Inayat, A; Sayed, E T; Shahbaz, M and Olabi, A G (2019). Improving the environmental impact of palm kernel shell through maximizing its production of hydrogen and syngas using advanced artificial intelligence. *Sci. Total Environ., 658*: 1150-1160. DOI: 10.1016/j.scitotenv.2018.12.284.

Russell, S and Norvig, P (2016). *Artificial Intelligence: A Modern Approach.* 3rd edition. Pearson, London. p. 744-748.

Sharifzadeh, M; Sadeqzadeh, M; Guo, M; Borhani, T N; Murthy Konda, N V S N; Garcia, M C; Wang, L; Hallett, J and Shah, N (2019). The multi-scale challenges of biomass fast pyrolysis and bio-oil upgrading: Review of the state of art and future research directions. *Prog. Energy Combust. Sci., 71*: 1-80. DOI: 10.1016/J.PECS.2018.10.006.

Smith, M B and March, J (2013). *March's Advanced Organic Chemistry: Reactions, Mechanisms and Structure*. 7th edition. John Wiley and Sons, New Jersey. 2080 pp.

Surahmanto, F; Saptoadi, H; Sulistyo, H and Rohmat, T A (2020). Investigation of the pyrolysis characteristics and kinetics of oil-palm solid waste by using Coats-Redfern method. *Energy Explor. Exploit., 38(1)*: 298-309. DOI: 10.1177/0144598719877759.

Teng, S Y; Loy, A C M; Leong, W D; How, B S; Chin, B L F and Máša, V (2019). Catalytic thermal degradation of *Chlorella vulgaris*: Evolving deep neural networks for optimization. *Bioresour. Technol., 292*: 121971. DOI: 10.1016/j.biortech.2019.121971.

Truhlar, D G (1978). Interpretation of the activation energy. *J. Chem. Educ., 55(5)*: 309.

Várhegyi, G; Antal Jr, M J; Jakab, E and Szabó, P (1997). Kinetic modeling of biomass pyrolysis. *J. Anal. Appl. Pyrolysis, 42(1)*: 73-87.

Vyazovkin, S; Burnham, A K; Criado, J M; Pérez-Maqueda, L A; Popescu, C and Sbirrazzuoli, N (2011). ICTAC kinetics committee recommendations for performing kinetic computations on thermal analysis data. *Thermochim. Acta, 520(1-2)*: 1-19.

Wang, B; Xu, F; Zong, P; Zhang, J; Tian, Y and Qiao, Y (2019). Effects of heating rate on fast pyrolysis behavior and product distribution of Jerusalem artichoke stalk by using TG-FTIR and Py-GC/MS. *Renew. Energy*, *132*: 486-496. DOI: 10.1016/j.renene.2018.08.021.

Wang, S; Dai, G; Yang, H and Luo, Z (2017). Lignocellulosic biomass pyrolysis mechanism: A state-of-the-art review. *Prog. Energy Combust. Sci., 62*: 33-86. DOI: 10.1016/J.PECS.2017.05.004.

Wang, X; Li, D; Yang, B; Liu, Y and Li, W (2013). Pyrolysis characteristics and kinetics of bamboo. *J. Biobased Mater. Bioenergy, 7(6)*: 702-707.

Wei, L; Xu, S; Zhang, L; Zhang, H; Liu, C; Zhu, H and Liu, S (2006). Characteristics of fast pyrolysis of biomass in a free fall reactor. *Fuel Process. Technol., 87(10)*: 863-871.

Yıldız, Z; Uzun, H; Ceylan, S and Topcu, Y (2016). Application of artificial neural networks to co-combustion of hazelnut husk-lignite coal blends. *Bioresour. Technol., 200*: 42-47. DOI: 10.1016/j.biortech.2015.09.114.

Zhang, J; Liu, J; Evrendilek, F; Zhang, X and Buyukada, M (2019). TG-FTIR and Py-GC/MS analyses of pyrolysis behaviors and products of cattle manure in CO_2 and N_2 atmospheres: Kinetic, thermodynamic, and machine-learning models. *Energy Convers. Manag., 195*: 346-359. DOI: 10.1016/j.enconman.2019.05.019.

Zhang, W; Zhang, J; Ding, Y; He, Q; Lu, K and Chen, H (2021). Pyrolysis kinetics and reaction mechanism of expandable polystyrene by multiple kinetics methods. *J. Clean Prod., 285*: 125042. DOI: 10.1016/j.jclepro.2020.125042.

Zhu, X; Li, Y and Wang, X (2019). Machine learning prediction of biochar yield and carbon contents in biochar based on biomass characteristics and pyrolysis conditions. *Bioresour. Technol., 288*: 121527. DOI: 10.1016/j.biortech.2019.121527.